Spectrum Sensing in the TV White Spaces

Daniel Riviello, Roberto Garello
Dipartimento di Elettronica e Telecomunicazioni
Politecnico di Torino
Torino, Italy
Email: {daniel.riviello, roberto.garello}@polito.it

Sergio Benco, Floriana Crespi, Alberto Perotti
Networks and Wireless Communications
CSP-ICT Innovation
Torino, Italy
Email: {sergio.benco, floriana.crespi, alberto.perotti}@csp.it

***Abstract*—Cognitive radio networks operating in the digital television white spaces are of particular interest for their practical applications. In this paper, we review several parametric and non-parametric test statistics commonly used in spectrum sensing. Both single-antenna as well as multiple antenna techniques are considered. For a selected subset of these techniques, an accurate performance assessment is carried out in the presence of a DVB-T primary signal generated using a software-defined real-time transmitter. Sensing performance is assessed both through Monte Carlo simulation and using a real *software-defined radio* implementation. Different channel profiles are considered. The obtained results show the performance of each algorithm in terms of detection probability under fixed false alarm rate and of *Receiver Operating Curve* (ROC). Moreover, these results permit to establish clear relationships between the considered algorithms in case of DVB-T primary signals.**

Keywords-Cognitive radio networks; spectrum sensing; white spaces; software-defined radio; DVB-T; eigenbased detectors.

I. Introduction

The following paper is an extended version of a previous work that the same authors presented at COCORA 2013 [1]. Here, a wider analysis is performed and a broader set of results is shown.

The ever increasing demand for higher data rates in wireless communications is strongly driving the search for new communication technologies able to exploit transmission opportunities wherever available. Unused channels in licensed radio-frequency (RF) bands, like those assigned to TV broadcasters, are one of the most attractive opportunities, since these enjoy favorable propagation conditions and feature fairly large bandwidths. As a matter of fact, some of the most relevant developments in this context are aimed at exploiting the so-called *TV white spaces* to provide broadband Internet access or other kind of wireless services through high-speed wireless communications carried out in the unused TV channels.

The cognitive radio concept [2] has been readily applied to TV white spaces networks and today white-space cognitive systems are one of the most active research fields in cognitive radio networks.

Some of the fundamental features and requirements of white-space cognitive systems include their ability to avoid interference to those who hold the right to use a certain band (the Primary Users, PU), while simultaneously performing high-speed communications. Such systems must as well be able to harmoniously coexist with other cognitive white-space systems (also called Secondary Users, SU) who operate on an non-interference basis with respect to PUs and may be operating in the same area. To these purposes, cognitive radio networks and the systems of which they are composed need to gain awareness of the surrounding electromagnetic environment. This is typically performed by using dedicated subsystems or relying on data provided by external entities.

Remarkable techniques used to gain said awareness include the access to geographically-referenced data bases containing spectral occupation information, *spectrum sensing* techniques, or a combination thereof. In this paper, we are mainly concerned with the investigation, analysis and performance evaluation of spectrum sensing techniques for white-space cognitive radio systems.

According to the cognitive radio paradigm, each node in a CR network must be equipped with an efficient *spectrum sensor* [3] a unit that makes the node able to gain awareness of the available transmission opportunities through the observation of the surrounding electromagnetic environment in a given range of frequencies. The sensor's ultimate goal consists in providing an indication to the node regarding whether a primary transmission is taking place in the observed channel. Such indication is determined as the result of a binary hypothesis testing experiment wherein hypothesis $\mathcal{H}_0$ ($\mathcal{H}_1$) corresponds to the absence (presence) of the primary signal. Thus, the sensing unit collects $1 \leq n \leq N$ samples of kind

$$y(n)|_{\mathcal{H}_0} = w(n) \quad (1)$$

$$y(n)|_{\mathcal{H}_1} = x(n) + w(n), \quad (2)$$

where $x(n)$ are samples of the primary signal as it is received by the spectrum sensor and $w(n)$ are noise samples.

Given the vector $y = (y(1), ..., y(n), ..., y(N)$ of acquired samples, the sensing algorithm computes a test statistics $T(y)$ and compares it against a predefined threshold θ. The performance of each detector is usually assessed in terms of *probability of detection* P_d and *probability of false alarm* P_{fa}

$$P_d = \mathbb{P}(T(y) > \theta|\mathcal{H}_1) \quad (3)$$

$$P_{fa} = \mathbb{P}(T(y) > \theta|\mathcal{H}_0), \quad (4)$$

as a function of the signal-to-noise ratio (SNR) ρ, which is defined as

$$\rho = \frac{\mathbb{E}\|x(n)\|^2}{\mathbb{E}\|w(n)\|^2}. \quad (5)$$

Several methods have been proposed for the computation of the test statistics: a comprehensive description can be found in [4] and references therein. In this paper, we consider a subset that includes most of the widely used algorithms: energy detection, multi-antenna eigenvalue based techniques, either under known or unknown noise variance hypothesis, and techniques exploiting specific signal characteristics, like the lagged-autocorrelation technique used to detect the cyclic prefix of OFDM signals [5][6][7].

Non-parametric methods are generally applicable to any kind of primary signal, since these methods do not make any assumption on the characteristics of such signal. Parametric methods, instead, assume a partial knowledge of some of the primary signal characteristics. The parametric method herein considered (lagged autocorrelation) has been applied to OFDM signals with cyclic prefix, but it can be straightforwardly applied to any other kind of cyclostationary signal, i.e., to almost all digitally modulated signals.

The main contributions of this paper are (i) an introductory review of the most relevant spectrum sensing algorithms, (ii) the application of such algorithms to real DVB-T signals generated using a software-defined real-time transmitter [8], (iii) the application of different realistic channel profiles and (iv) the complexity assessment performed through the software-radio implementation of the considered sensing algorithms. The algorithms' performance and complexity are evaluated and compared in realistic conditions, providing useful results for practical realizations.

II. Primary signal

The DVB-T standard [9] specifies a set of coded OFDM transmission schemes to be used for broadcasting of multiplexed digital television programs.

The transmitted signal consists of a sequence of fixed-duration OFDM symbols. A cyclic prefix (CP) is prepended to each symbol in order to avoid inter-symbol interference over frequency-selective fading channels. The most relevant parameters of DVB-T signals are shown in Table I.

The signal bandwidth is approximately 7.61 MHz, with an intercarrier frequency spacing of 8MHz. A subset of the available 2048 subcarriers (in 2k mode) or 8192 subcarriers (in 8k mode) are used to carry higher layer data and PHY-layer signalling information. The latter consists of pilot sequences, either allocated to fixed subcarriers (continual pilots) or scattered throughout OFDM symbols according to a periodic pattern, which are used for channel estimation at the receiver side, and Transmission Parameter Signaling (TPS) information, wherein encoded information about the current transmission parameters used on data subcarriers is delivered.

OFDM symbols with CP are grouped into frames and superframes: each frame consists of 68 symbols and each superframe consists of 4 frames.

In our study, we used a real encoded and modulated MPEG transport stream (TS) with code rate 5/6, 64-QAM constellation and CP ratio 1/4. The resulting bit rate is approx. 24.88 Mbits/s. At the sensing unit, the DVB-T signal was sampled at the nominal rate of 64/7 Msamples/s.

TABLE I
Main parameters of DVB-T.

	2k mode	8k mode
Symbol duration (T_U)	$224\mu s$	$896\mu s$
Guard interval duration (Δ)	$7-56\mu s$	$28-224\mu s$
Number of active subcarriers	1705	6817
Subcarrier spacing (approx.)	4464Hz	1116Hz
CP duration ratio (Δ/T_U)	1/4, 1/8, 1/16, 1/32	
Constellations	QPSK, 16-QAM, 64-QAM	
Code rate	1/2, 2/3, 3/4, 5/6, 7/8	

A. DVB-T signal characteristics

As a common assumption in the literature on spectrum sensing, the primary signal is modeled as a Gaussian process. Fig. 1 shows that, in the case of DVB-T signals, this assumption is well motivated. In fact, Fig. 1(a) shows the *pdf* of the real and imaginary parts of the DVB-T signal's complex envelope. Clearly, the Gaussian distribution is very well approximated. A more accurate evaluation is provided in Fig. 1(b), where the *quantile-quantile* plot of the DVB-T distribution vs. a zero-mean Gaussian distribution with same variance is shown.

B. Channel characteristics

Let us assume that the primary signal is detected through K sensors (receivers or antennas). Let $\boldsymbol{y}(n) = [y_1(n) \dots y_k(n) \dots y_K(n)]^T$ be the $K \times 1$ received vector at time n, where the element $y_k(n)$ is the n-th discrete baseband complex sample at receiver k.

Typically, a flat Rayleigh fading channel is considered in the literature. In such case, the received signal can be modeled as a linear mixture model of kind

$$\boldsymbol{y}(n) = \boldsymbol{h}x(n) + \boldsymbol{v}(n), \tag{6}$$

where $\boldsymbol{h}$ is the K-element channel vector of size $K \times 1$ whose elements $h_n \sim N_{\mathbb{C}}(0, \sigma_h^2)$ are mutually independent. Moreover we apply the following normalization:

$$\sum_{n=1}^{K} h_n h_n^* = K. \tag{7}$$

Moreover, $\boldsymbol{v}(n)$ is the additive white Gaussian noise distributed as $N_{\mathbb{C}}(\mathbf{0}_{K\times 1}, \sigma_v^2 \mathbb{I}_{K\times K})$.

In order to assess the performance of the considered algorithms in a more realistic case, we used a frequency- and time-selective channel model, the 6-path Typical Urban (TU6) mobile radio propagation model developed by the COST 207 European project [10]. This profile is a frequency- and time-selective Rayleigh fading channel model. Given $x(t)$ and $y(t)$ the input and output signal respectively, it can be expressed as follows:

$$y(t) = \sum_{i=1}^{M} \gamma_i e^{-j\theta_i} x(t - \tau_i), \tag{8}$$

where:

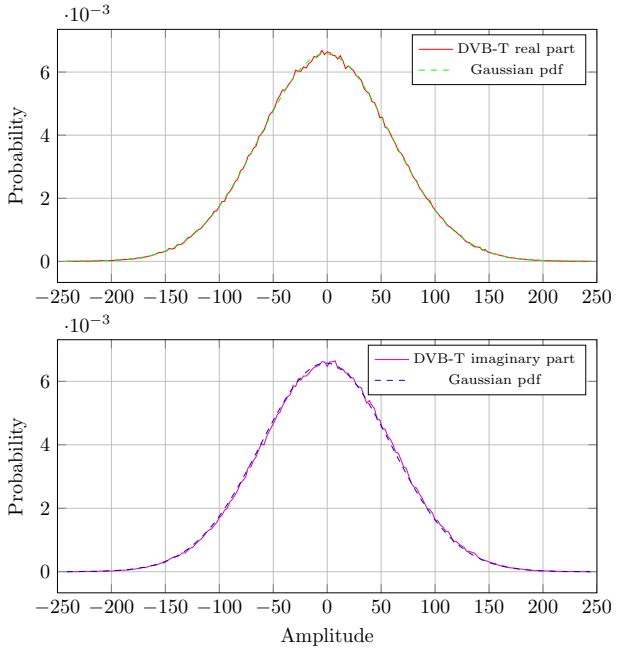

(a) Estimated probability density function.

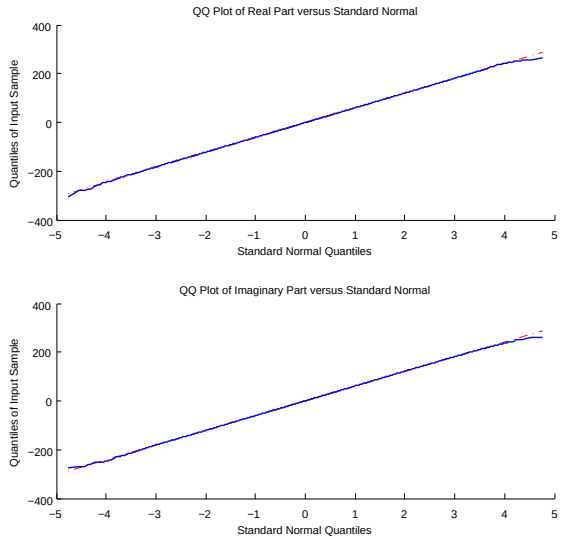

(b) Quantile-quantile plot.

Fig. 1. Statistics of the DVB-T signal.

- M is the number of paths equal to 6;
- γ_i is the average path gain of the ith path (listed in Tab. II-B);
- θ_i is the phase shift from scattering of the i'th path, modeled as a uniformly distributed random variable in $[-\pi, \pi]$;
- τ_i is the relative delay of the ith path (listed in Tab. II-B);

where the classical doppler spectrum is defined as:

$$G(f; f_D) = \frac{1}{\sqrt{1-(f/f_D)^2}}. \quad (9)$$

In our simulation the Doppler spread f_D has been set to 10 Hz, corresponding to a pedestrian mobile profile.

TABLE II
TYPICAL URBAN PROFILE (TU6).

Tap number	Delay τ_i (μs)	Average gain γ_i (dB)
1	0.0	-3
2	0.2	0
3	0.5	-2
4	1.6	-6
5	2.3	-8
6	5.0	-10

III. TEST STATISTICS

As explained in the previous section, the detector builds its test statistic from K sensors (receivers or antennas) and N time samples. The symbol $\boldsymbol{y}(n) = [y_1(n) \dots y_k(n) \dots y_K(n)]^T$ denotes the $K \times 1$ received vector at time n, where the element $y_k(n)$ is the n-th discrete baseband complex sample at receiver k.

The noise is modeled as an additive white Gaussian noise process with zero mean and variance $\sigma_v^2 = N_0/2$, N_0 being the two-sided power spectral density of noise.

The received samples are stored in a $K \times N$ matrix:

$$\boldsymbol{Y} \triangleq [\boldsymbol{y}(1) \dots \boldsymbol{y}(N)]. \quad (10)$$

The sample covariance matrix $\boldsymbol{R}$ is:

$$\boldsymbol{R} \triangleq \frac{1}{N} \boldsymbol{Y}\boldsymbol{Y}^H. \quad (11)$$

We will denote by $\lambda_1 \geq \dots \geq \lambda_K$ the eigenvalues of $\boldsymbol{R}$, sorted in decreasing order.

The usual criterion for comparing two tests is to fix the false alarm rate P_{fa} and look for the test achieving the higher P_d . The Neyman Pearson (NP) lemma [11] is known to provide the Uniformly Most Powerful (UMP) test, achieving the maximum possible P_d for any given value of P_{fa} . The NP criterion is applicable only when both $\mathcal{H}_0$ and $\mathcal{H}_1$ are simple hypotheses. In our setting this is the case when both the noise level σ_v^2 and the channel vector $\mathbf{h}$ are a priori known. The NP test is given by the following likelihood ratio:

$$T_{NP} = \frac{p_1(\mathbf{Y}; \mathbf{h}, \sigma_s^2, \sigma_v^2)}{p_0(\mathbf{Y}; \sigma_v^2)}. \quad (12)$$

For the considered model, the expressions of p_0 and p_1 can be found in [12]. The NP test provides the best possible performance, but requires exact knowledge of both h and σ^2. For most practical applications, the knowledge of h is questionable. The noise variance is somewhat easier to know: since we only consider thermal noise, if the temperature is constant some applications may possess an accurate estimation of it.

Many spectrum sensing algorithms have been proposed in the literature. Reviews and comparisons can be found, for example, in [4][13][14]. In this paper, we consider some of the most popular tests, with the aim of comparing them against true DVB-T signals. The considered tests are divided in three classes.

A. Non-parametric tests, known noise variance

These tests are non-parametric, i.e., do not exploit the knowledge of the signal characteristics. An excellent estimation of the noise variance σ_v^2 is supposed (obtained, for example, during a long training phase).

Roy's Largest Root Test (RLRT): this method tests the largest eigenvalue of the sample covariance matrix against the noise variance. The test statistic is

$$T_{RLRT} = \frac{\lambda_1}{\sigma_v^2}. \quad (13)$$

The RLRT was originally developed in [15]. Performance analysis can be found, for example, in [16][17][14].

Under $\mathcal{H}_1$, the asymptotic behavior of λ_1/σ_v^2 has a *phase transition phenomenon* [18], which depends on the SNR. In case of a single signal the critical value can be expressed as [19]:

$$\rho_{\text{crit}} = \frac{1}{\sqrt{KN}}. \quad (14)$$

If the SNR ρ is lower than the critical value, the limiting distribution of λ_1/σ_v^2 is the same as that of the largest noise eigenvalue, thus nullifying the statistical power of a largest eigenvalue test. If the SNR is higher, the largest eigenvalue λ_1 depends on the signal plus noise power, while the smallest $K1$ eigenvalues depends on the noise only. The optimality of RLRT in the class of "semi-blind" algorithms was pointed out in [17]. For a single emitting source, if the SNR is above the identifiability threshold given by (14), the signal is detectable by the largest eigenvalue λ_1 value. Starting from the NP test and using the asymptotic expansion of the hypergeometric function, it was shown in [17] that, under known noise variance, distinguishing between $\mathcal{H}_0$ and $\mathcal{H}_1$ in the asymptotic regime ($N \to \infty$ with K fixed) depends to leading order only on λ_1. For Gaussian signals and not too low signal-to-noise ratio, the RLRT is the best test statistics in this class.

Energy Detection (ED): the test statistic is the average energy of the received samples, normalized by the noise variance:

$$T_{ED} = \frac{1}{KN\sigma_v^2} \sum_{k=1}^{K} \sum_{n=1}^{N} |y_k(n)|^2 . \quad (15)$$

The energy detection method is probably the most popular technique for spectrum sensing, also thanks to its simplicity. Analytical performance expressions for this detector are well-known in the literature (e.g., [20]).

Likelihood Ratio Tests (LRT): different LRT-based detectors were given in [13]. The complete, noise-dependent, log-likelihood ratio test statistic is given by

$$T_{LRT} = 2(N-1)\left[\log\left(\frac{\sigma_v^{2K}}{\det \boldsymbol{R}}\right) + \left(\frac{\text{tr}\boldsymbol{R}}{\sigma_v^2} - K\right)\right]. \quad (16)$$

Performance analysis for this test can be found, for example, in [13].

B. Non-parametric tests, unknown noise variance

These tests are again non-parametric, but the noise variance is supposed unknown.

Generalized Likelihood Ratio Test (GLRT): this method uses as test statistic the ratio

$$T_{GLRT} = \frac{\lambda_1}{\frac{1}{K}\text{tr}(\boldsymbol{R})}. \quad (17)$$

Performance analysis can be found for example in [21].

The class of "blind" detection tests includes all algorithms where the noise variance σ_v^2 is unknown and not used in the test statistic. It has been recently proved in [22] that the GLRT procedure is optimal, asymptotically and even for finite sample size, in a combined Neyman-Pearson/Bayesian sense, such that it minimizes the average mean-square parameter estimation error subject to an upper bound constraint on the false-alarm probability. Therefore, the GLRT detector [12] is indeed the best performing method in the blind eigenvalue-based class.

By a simple transformation, it is possible to relate GLRT to RLRT. We first note that, since

$$\frac{1}{T_{GLRT}} = \frac{\sum_{i=1}^{K}\lambda_i}{\lambda_1} = 1 + \frac{\sum_{i=2}^{K}}{\lambda_1}, \quad (18)$$

the GLRT is equivalent to

$$T'_{GLRT} = \frac{\lambda_1}{\frac{1}{K-1}\sum_{i=2}^{K}\lambda_i}. \quad (19)$$

In case of a single signal, the new denominator is the average of the noisy eigenvalues and can be interpreted as the Maximum-Likelihood (ML) estimate of the noise variance:

$$\hat{\sigma}_v^2 = \frac{1}{K-1}\sum_{i=2}^{K}\lambda_i. \quad (20)$$

As a consequence, we have obtained this equivalent formulation of the GLRT:

$$T'_{GLRT} = \frac{\lambda_1}{\hat{\sigma}_v^2}. \quad (21)$$

We can observe that the structure of RLRT (13) and GLRT (17) is very similar: RLRT uses the true noise variance, while GLRT uses its ML estimation computed within the sensing slot by using the noise eigenvalues.

Eigenvalue Ratio Detector (ERD): the test statistic (also called maximum-minimum eigenvalue, or condition number test) is the ratio between the largest and the smallest eigenvalue of $\boldsymbol{R}$

$$T_{ERD} = \frac{\lambda_1}{\lambda_K}. \quad (22)$$

Performance analysis can be found, for example, in [23][19].

Noise-independent LRT (LRT-): an alternative log-likelihood ratio was derived in [13], under the assumption of unknown noise variance:

$$T_{LRT-} = 2(N-1)\left[\frac{\frac{1}{K}\sum_{i=1}^{K}\lambda_i}{\left(\prod_{i=1}^{K}\lambda_i\right)^{1/K}}\right]^K. \quad (23)$$

In statistics, this method has been known for many years as the *sphericity test* [24][25]. Performance analysis for cognitive radio applications can be found, for example, in [13].

C. Detectors based on cylic prefix autocorrelation

Primary signal detectors that exploit the presence of the cyclic prefix (CP) in OFDM transmissions have been proposed in the literature. In [5], the detectors based on CP correlation described in [6] have been improved, applied to a real scenario and implemented using a software-defined radio (SDR) platform.

As previously stated, a DVB-T signal consists of OFDM-modulated symbols of which a-priori knowledge of transmission parameters is assumed: the number of subcarriers, cyclic prefix length, constellation type and the code rate. The aim of parametric test statistics is to exploit the knowledge of signal parameters (i.e., signal features) in order to improve primary signals detection with high sensitivity.

The algorithm implemented in [5] using SDR is the well known CP-based spectrum sensing. Assuming that each OFDM symbol consists of $N_s = N_c + N_d$ samples (where N_c is the number of samples in the cyclic prefix and N_d is the number of data samples), the CP correlation function (Eq. 3 in [5]), becomes:

$$R_{xx}^{(\mathrm{CP})}[\tau] = \frac{1}{KN_s}\left|\sum_{k=0}^{K-1}\sum_{n=\tau-kN_s}^{\tau-kN_s-N_c+1} x^*[n]x[n-N_\mathrm{d}]\right|. \quad (24)$$

where K is the number of OFDM symbols on which we compute coherent averaging and τ represents the synchronization mismatch between our acquisition and the symbol start.

The coherent averaging taking the absolute value allows us to improve sensitivity in presence of AWGN noise at the cost of a larger observation interval.

Moreover, to enable the practical implementation of these algorithms, it is necessary to define a noise estimation algorithm to set a threshold that guarantees certain detection performance in terms of probability of false alarm (P_{fa}) and probability of detection (P_d). A slight improvement in terms of noise estimation accuracy (i.e., correlation noise) with respect to [5] is obtained by devising a suitable noise level estimator: without any a-priori knowledge, the correlation noise estimation should be performed by analyzing the received samples when the H_0 hypothesis is true. Hence, training periods with only noise samples must be performed periodically (e.g., to track system temperature changes). To avoid dedicated training, we observed that noise samples can be gathered in a suitable interval between two consecutive correlation maxima. The correlation function $\tilde{R}$ used to estimate the average correlation noise level correspond to the function R, excluding $2N_c$ samples around the detected maxima. In these intervals, $\tilde{R}(\tau) = 0$.

Our optimized CP-based algorithm can thus be summarized as follows:

1) Receive K(N_c+N_d)+N_d samples
2) Perform (24) over acquired samples
3) Record the correlation maximum and its index i
4) Copy only correlation noise values from function in 2. excluding values that have index in the range $i - N_c < i < i + N_c$
5) Decide if the channel is occupied by evaluating the following metric:

$$\frac{\max R_{xx}^{(CP)}[\tau]}{\mathrm{avg}\tilde{R}_{xx}^{(CP)}[\tau]} \gtrless \gamma. \quad (25)$$

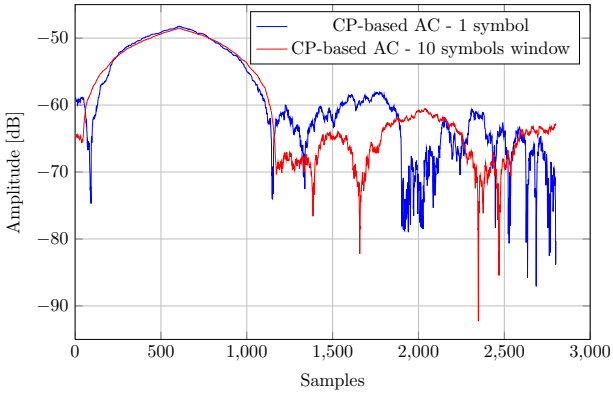

Fig. 2. Amplitude of the CP-based auto-correlation - 1 symbol vs. 10 symbols observation.

Fig. 2 shows the amplitude of the CP-based autocorrelation function with an observation window of respectively $K = 1$ and $K = 10$ symbols in an ideal channel scenario (infinite SNR, no thermal noise). It can be observed that, for $K = 10$, the ratio of the peak value over the maximum value observed outside the cyclic prefix window is improved with respect to $K = 1$.

IV. GNU Radio Implementation

The SDR concept has been introduced almost twenty years ago in [26] and it is innovative even nowadays. The main scope of SDR is to improve the flexibility of radio communication devices by implementing the digital sections entirely in software using dedicated or general-purpose processors.

Different SDR platforms have been developed in recent and past years. Among these, an open platform called GNU Radio has prevailed firstly in the academic community and it is becoming frequently adopted even in industrial projects. GNU Radio is a free and open-source software development toolkit for the SDR implementation of transceivers [27]. GNU Radio is not primarily a simulation tool, although it can be used for this purpose. When paired with suitable RF front-ends, a real radio transceiver can be realized. Typically, GNU Radio uses, as RF front-end, the Universal Software Radio Peripheral (USRP) devices by Ettus Research. The GNU Radio environment is structured as a layer of C++ classes organized in components: the *gnuradio-core* component includes a scheduler able to orchestrate the execution of signal processing blocks. Transceiver systems can be modeled through a flow graph, i.e., a set of interconnected signal processing blocks that

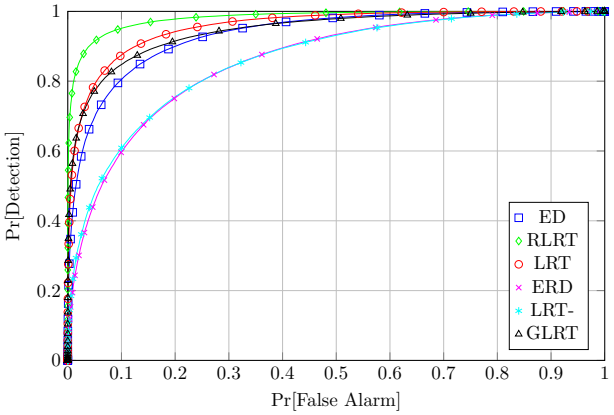

(a) Receiver operating curves (SNR = -10dB).

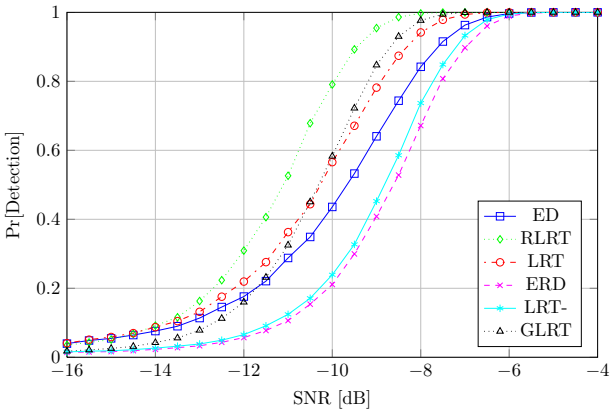

(b) Detection probability.

Fig. 3. DVB-T signal through flat-fading channel.

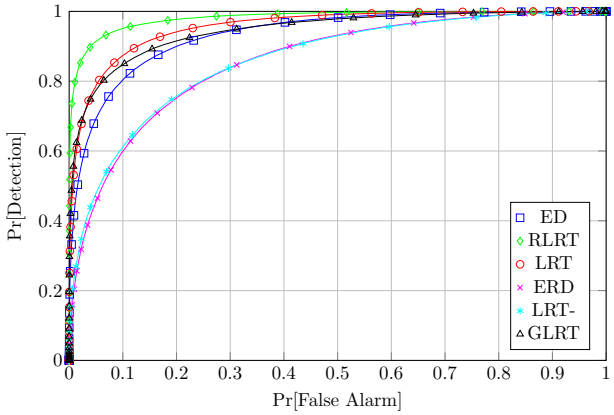

(a) Receiver operating curves (SNR = -10dB).

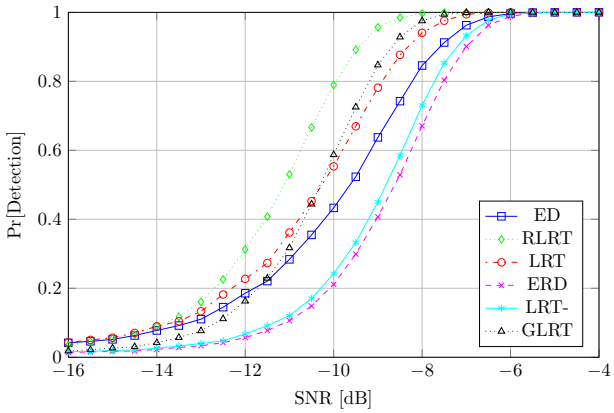

(b) Detection probability.

Fig. 4. Gaussian signal through flat-fading channel.

the scheduler executes. Concerning the software structure, it is possible to define models using a high-level object-oriented language such as Python, thanks to an interfacing layer, the Simple Wrapper and Interface Generator (SWIG), that permits to call methods of classes written in C++ from Python. The GNU Radio blocks can be connected to each other to form a flow graph either by using Python or C++, which would result in a higher efficiency. Finally, a graphical tool called GNU Radio Companion (GRC) can be used to compose flow graphs in a visual environment. GRC makes use of the eXtensible Markup Language (XML) to store the flow graph designs. The GNU Radio core components and libraries make available several basic and advanced signal processing and math blocks that make the implementation of transceivers much faster. Users can create new blocks to implement new algorithms that have not been developed yet.

A. *Signal processing blocks*

A module identifies a structure, which is possible to integrate in the overall GNU Radio framework. It consists of one or more signal processing blocks implemented as C++ classes with a well-defined interface.

The main section of a signal processing block is its C++ core engine. The design of a block starts with the definition of the input and output ports, their data types and multiplicities. These characteristics are defined in the block “signature”. A constructor (the “make” method) contains all the initialization code. The sample rates of input and output ports are, in general, different, although some constraints are imposed by some framework design choices. A difference in sample rates between input and output must be notified to the runtime component by calling the “forecast” method, which tells the scheduler how many input items are required to produce a given number of output items. The main signal processing algorithm is defined in the “general_work” method. It receives the data stream provided by the runtime through its input ports, processes it generating output items that are forwarded to blocks connected to its output ports.

Special types of blocks are the sink and source. These are characterized by the lack of either input or output ports. Each flow graph must contain at least one source block and one sink block. As an example, a special sink block is used to connect the flow graph to a USRP device, which will be used to transmit the radio signal.

V. EIGENBASED DETECTOR BLOCK

The two optimal non-parametric tests, RLRT and GLRT, respectively for the class of “semi-blind” and “blind” detec-

tors, have been implemented and tested in the GNU Radio platform.

A. Eigenvalue algorithm

The most significant part of the GNU Radio block consists in the computation of eigenvalues of the covariance matrix $\boldsymbol{R}$. Such computation is performed through 2 stages: the Lanczos algorithm and the bisection method.

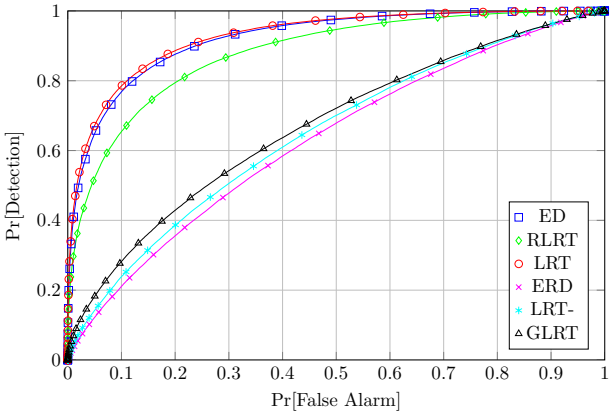

(a) Receiver operating curves (SNR = -10dB).

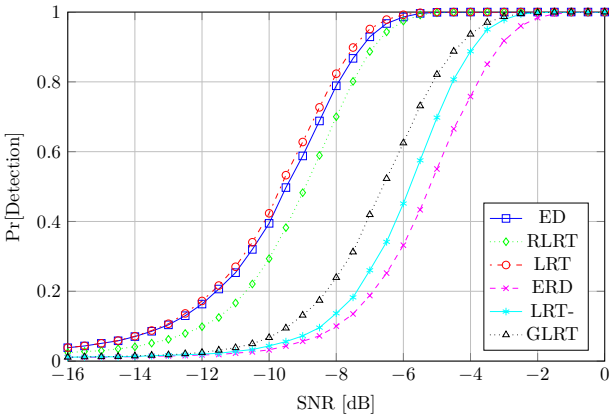

(b) Detection probability.

Fig. 5. DVB-T signal through TU6 channel.

1) Lanczos algorithm: In order to choose the best possible solution we have to take into account that the covariance matrix $\boldsymbol{R}$ is Hermitian, hence the Lanczos method can be applied.

The Lanczos algorithm can be viewed as a simplified Arnoldi's algorithm [28] in that it applies to Hermitian matrices. In the algorithm a series of orthonormal vectors, $\boldsymbol{q}_1, \ldots, \boldsymbol{q}_n$, is generated, which satisfy:

$$\boldsymbol{T} = \boldsymbol{Q}^T \boldsymbol{R}\, \boldsymbol{Q}. \tag{26}$$

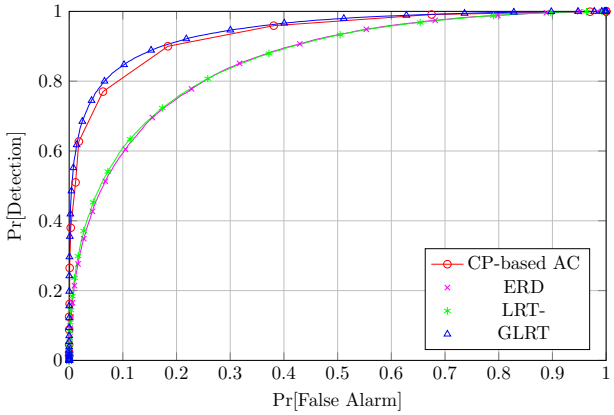

(a) Receiver operating curves (SNR = -10dB).

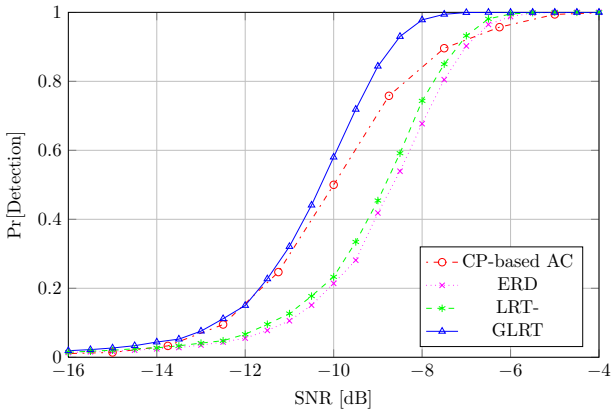

(b) Detection probability.

Fig. 6. Comparison with the CP correlation method.

The matrix $\boldsymbol{T}$ is tridiagonal:

$$\boldsymbol{T}_j = \begin{pmatrix} \alpha_1 & \beta_2 & & & & 0 \\ \beta_2 & \alpha_2 & \beta_3 & & & \\ & \beta_3 & \alpha_3 & \ddots & & \\ & & \ddots & \ddots & \beta_{j-1} & \\ & & & \beta_{j-1} & \alpha_{j-1} & \beta_j \\ 0 & & & & \beta_j & \alpha_j \end{pmatrix},$$

the iterative procedure is based on this three-term recurrence relation:

$$\beta_{j+1}\, \boldsymbol{q}_{j+1} = \boldsymbol{R}\, \boldsymbol{q}_j - \alpha_j\, \boldsymbol{q}_j - \beta_j\, \boldsymbol{q}_{j-1}. \tag{27}$$

More details on the procedure can be found in [29][30]. Here is a short description of the simulation algorithm in pseudocode:

```
1: function LANCZOS(R, K)
2:     q_1 uniformly distributed random vector
3:     q_1 = q_1/||q_1||
4:     α_1 = q_1^H R q_1
5:     w_1 = R q_1 − α_1 q_1
6:     β_1 = 0
7:     β_2 = ||w_1||
8:     for i = 2 → K do
9:         q_i = w_{i−1}/β_i
```

```
        α_i = q_i^H R q_i
        w_i = R q_i − α_i q_i − β_i q_{i−1}
        if i < K then
            β_{i+1} = ||w_i||
        end if
    end for
end function
```

The main problem of Lanczos algorithm is the stability, using floating point arithmetic the orthogonality of the vectors $\boldsymbol{q}_j$ is quickly lost. Several stable orthogonalization schemes have been proposed, such as [31], although none of these methods have been applied in our GNU Radio block, since we are basically interested in the computation of the maximum eigenvalue of the covariance matrix. In fact, even with such loss of orthogonality, the algorithm generates very good approximations of the largest eigenvalue. As proven in [32], the Lanczos algorithm produces faster and more accurate results than the power method.

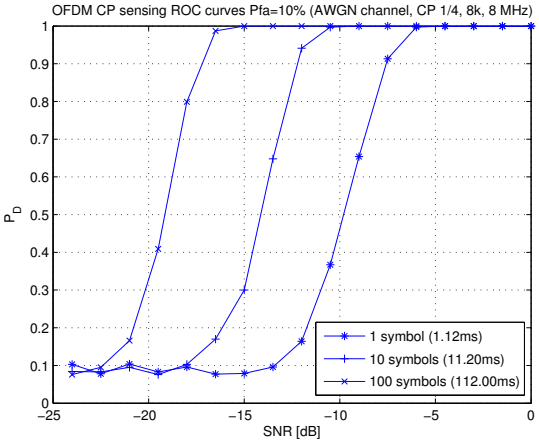

Fig. 7. CP based algorithm probability of detection curves considering a different number of consecutive OFDM symbols.

2) Bisection algorithm: Once, after K iterations, the tridiagonal matrix T has been obtained, the maximum eigenvalue can be simply computed through the bisection algorithm (also called spectral bisection). The algorithm is an iterative procedure based on the computation of the modified Sturm sequence, as explained in [33][34]. The original Sturm sequence, for any number c, is based on the following recursive relation:

$$\begin{aligned} p_0(c) &= 1 \\ p_1(c) &= \alpha_1 - c \\ p_i(c) &= (\alpha_i - c)p_{i-1}(c) - \beta_i^2 p_{i-2}(c), \end{aligned} \tag{28}$$

where $[\alpha_1, \ldots, \alpha_K]$ and $[\beta_2, \ldots, \beta_K]$ are respectively the diagonal and off-diagonal elements of the matrix $\mathbf{T}$. The number $f(c)$ of disagreements in sign between consecutive number of the sequence is equal to the number of eigenvalues smaller than c. However, the original sequence suffers from underflow and overflow problems in floating-point arithmetic, thus, the original sequence $p_i(c)$ is replaced by the sequence $q_i(c)$ defined as

$$q_i(c) = p_i(c)/p_{i-1}(c), \tag{29}$$

now the number of eigenvalues smaller than c, $f(c)$ is given by the number of negative $q_i(c)$. Hence, the new recursive relation is:

$$\begin{aligned} q_1(c) &= \alpha_1 - c \\ q_i(c) &= (\alpha_i - c) - \beta_i^2/q_{i-1}(c). \end{aligned} \tag{30}$$

The algorithm implemented in the GNU Radio block is a slightly modified version of the bisection method described in [33], which computes only the largest eigenvalue. The first part of the algorithm exploits the Gershgorin circle theorem to estimate the upper and lower bounds of the eigenspectrum of the matrix $\mathbf{T}$. In the following pseudocode the bisection function has 6 parameters:

- $\boldsymbol{\alpha}$: diagonal elements of the matrix $\mathbf{T}$;
- $\boldsymbol{\beta}$: off-diagonal elements of $\mathbf{T}$;
- K: order of the tridiagonal matrix;
- m: eigenvalue λ_m is computed, in this algorithm λ_K is the largest eigenvalue (opposite notation w. r. t. III), so $m = K$;
- γ: required precision for the computation of the eigenvalue, which affects the number of iterations;
- ϵ: machine epsilon, the smallest number for which $1+\epsilon > 1$ in the computer.

```
function BISECTION(α, β, K, m, γ, ε)
    xmin = α_K − |β_K|
    xmax = α_K + |β_K|
    for i = K − 1 → 1 do
        h = |β_i| + |β_{i+1}|
        if α_i + h > xmax then
            xmax = α_i + h
        end if
        if α_i − h < xmin then
            xmin = α_i − h
        end if
    end for
    u = xmax
    x = xmax
    v = xmin
    while (u − v) > 2ε(|v| + |u| + γ) do
        p = (u + v)/2
        a = 0
        q = 1
        for i = 1 → K do
            if q ≠ 0 then
                q = α_i − p − β_i^2/q
            else
                q = α_i − p − |β/ε|
            end if
            if q < 0 then
                a = a + 1
            end if
```

```
        end for
        if a < m then
            v = p
        else
            u = p
        end if
    end while
    x = (u + v)/2
    return x
end function
```

B. Description of the "eigenbased" block

In order to work in the GNU Radio framework, the eigenbased detector required the development of a new GNU Radio block. All the details and guidelines on how to write a block can be found, for example, in [35]. Fig. 8 shows the "eigenbased" block.

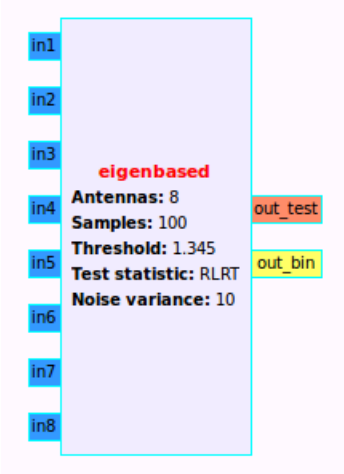

Fig. 8. "Eigenbased" GNU Radio block.

The block has been developed in C++, furthermore a very short part of code has been written in Python and XML in order to make the block available in GNU Radio Companion. The eigenvalue algorithm has been successfully tested in a standalone C++ program up to $K = 100$, while in GNU Radio, for real-time computational effort reasons, we limited K and consequently the block input ports to 32. For simplicity we have shown in Fig. 8 an 8-port block. Since we usually deal with complex baseband signals, all the input must be of type complex.

Five parameters can be set by the user:

- *Antennas*: it corresponds to K, the number of sensors or the oversampling factor in case of single receiving antenna.
- *Samples*: it corresponds to N, the number of samples stored on each row of the Y matrix.
- *Threshold*: the test statistic is compared against this value.
- *Test statistic*: it can be chosen between RLRT or GLRT.
- *Noise variance*: this is required only for RLRT.

The output ports are described as follows:

- *out_test*: type float, it's the floating point value of the computation of the test statistic.
- *out_bin*: type short, after comparing the test statistic against the threshold, it is equal to 1 if the *out_test* is larger than the threshold or equal to 0 otherwise.

VI. CP-BASED DETECTOR BLOCK

A well-known class of techniques that exploits a-priori knowledge of parameters of the received signal is the so-called feature-based detectors. In this subsection, an SDR implementation of an OFDM feature-based detector is discussed.

In order to enable fast symbol synchronization and also avoid inter-symbol interference, the OFDM modulation provides a Cyclic Prefix (CP) insertion between consecutive symbols. Every CP is obtained by copying the tail portion of the OFDM symbol before its head, thus performing a cyclic extension. The result is that the CP length uniquely characterizes each OFDM-based standard. The DVB-T standard, for example, provides four different CP lengths: 1/4, 1/8, 1/16, 1/32 of the OFDM symbol duration. The repetitive pattern produced by the CP can be detected using the CP autocorrelation function (24). Using GNU Radio and the USRP2, the CP-based detection algorithm has been implemented and tested in a real scenario. The resulting spectrum sensing unit is capable of sampling the received signal at 12.5 MHz and calculating (24) to verify the presence of the Cyclic Prefix (CP). In [5], the detectors based on CP autocorrelation described in [6] have been implemented, improved, and applied to a real scenario. The implemented algorithm computes the accumulated autocorrelation function over K OFDM symbols (24) and the test statistics (25).

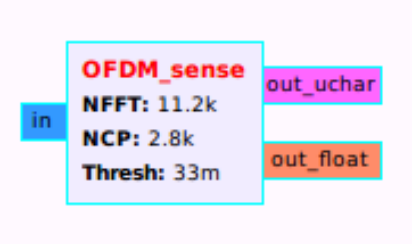

Fig. 11. "OFDM_sense" GNU Radio block.

The developed GNU Radio block, shown in Fig. 11 features the following parameters: number of data samples ($NFFT \equiv N_d$), the number of CP samples ($NCP \equiv N_c$) and the threshold value. The block features one input port through which the received signal is fed and two output ports through which the result of the test statistics is provided in two different numerical formats.

In this work, the USRP2 has been set to process a bandwidth of 12.5 MHz.

Since the DVB-T signal consists of a continuous flow of transmitted symbols, it is possible to perform the sample processing in two steps:

1) buffering;

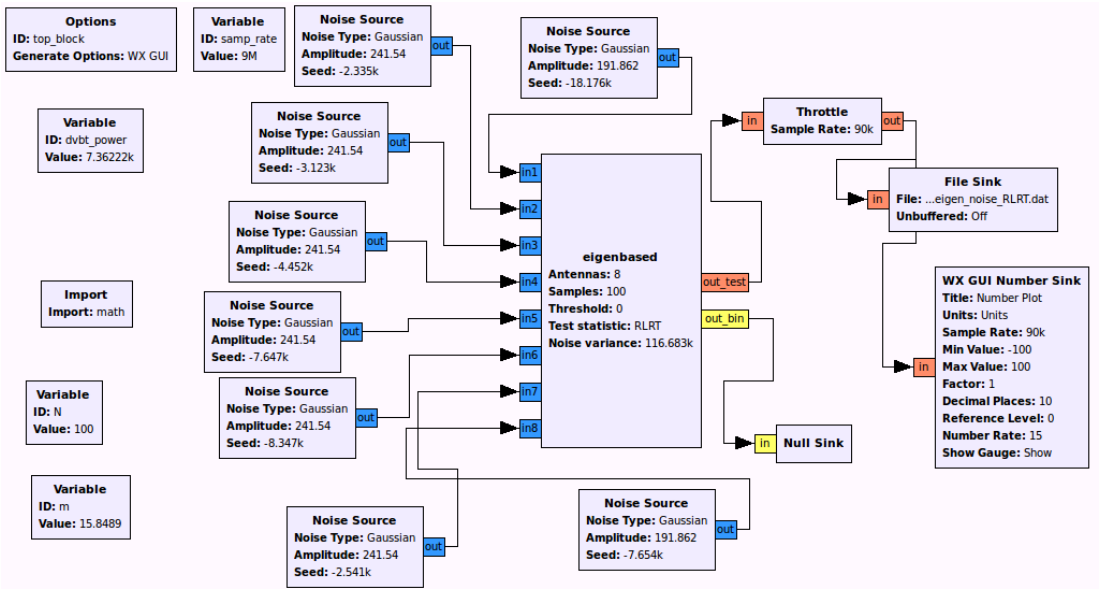

Fig. 9. GNU Radio flow graph corresponding to the $\mathcal{H}_0$ case.

2) compute CP autocorrelation.

This aims at keeping the system responsive and effective. The samples generated by the USRP2 are copied to the input buffer in the general work function that returns no samples until the input buffer is full. Once the buffer is ready, the input from USRP2 is temporarily paused and the processing starts. The samples processed in the general work function are sent at the first output port using a stream of floats. The second output port produces the estimated minimum correlation value, which will be used to set the threshold. A probe block is thus connected to the second output port in order to copy the correlation minimum to the threshold parameter.

VII. Simulation and Results

The performance of the algorithms have been assessed firstly through a numerical computing environment and then using the SDR platform GNU Radio. The performance of each algorithm is shown in terms of:

- the ROC (Receiver Operating Characteristic) curve obtained by plotting the detection probability versus the false alarm probability;
- the detection probability as a function of the signal-to-noise ratio, with fixed false alarm rate (typically, $P_{fa} = 0.01$).

A. Simulation procedure

The Monte Carlo method has been used for our simulation. In order to estimate the values of P_{fa} and P_d, $N_T = 10000$ trials have been performed for each SNR value.

For each considered detection algorithm, we computed the test statistics T_1 corresponding to $\mathcal{H}_1$ (signal plus noise) and T_0 corresponding to $\mathcal{H}_0$ (noise). The estimated P_{fa} (resp. P_d) value corresponding to a given threshold θ is then computed as the empirical complementary cumulative distribution of T_0 (resp. T_1) at θ.

Here is a short description of the simulation algorithm in pseudocode:

$N_B = 1000$ ▷ N_B = number of threshold values
for all *SNR* values **do**
  for $i = 1 \rightarrow N_T$ **do**
    for all detectors **do**
      compute signal+noise test statistic $T_1(i)$
      compute only-noise test statistic $T_0(i)$
    end for
  end for
  for all detectors **do**
    create vector of thresholds $\boldsymbol{\theta}$ of N_B equally spaced values from min($\boldsymbol{T_0}$) to max($\boldsymbol{T_1}$)
    create vector of N_B elements $\boldsymbol{P_{fa}}$
    create vector of N_B elements $\boldsymbol{P_d}$
    for $i = 1 \rightarrow N_B$ **do**
      for $j = 1 \rightarrow N_T$ **do**
        if $T_0(j) > \theta(i)$ **then**
          $P_{fa}(i) \leftarrow P_{fa}(i) + 1$
        end if
        if $T_1(j) > \theta(i)$ **then**
          $P_d(i) \leftarrow P_d(i) + 1$
        end if
      end for
      $P_{fa}(i) \leftarrow P_{fa}(i)/N_T$
      $P_d(i) \leftarrow P_d(i)/N_T$
    end for
  end for
end for

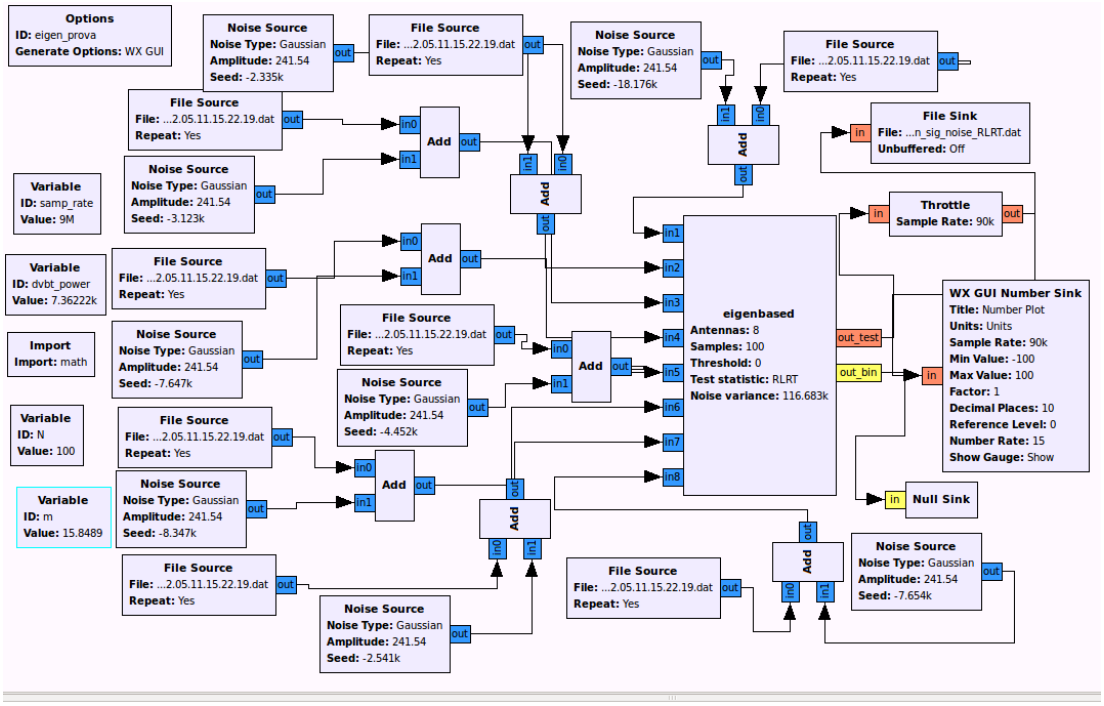

Fig. 10. GNU Radio flow graph corresponding to the $\mathcal{H}_1$ case.

B. GNU Radio flow graphs

At a later stage, we assessed the performance of the algorithms using SDR tools. We defined two different flow graphs containing the "eigenbased" block shown in Fig. 8. In the first flow graph (Fig. 9), corresponding to $\mathcal{H}_0$, only noise sources have been connected to the "eigenbased" block inputs. This configuration has been used to set the threshold θ according to a fixed value of P_{fa}.

In the second flow graph, (corresponding instead to $\mathcal{H}_1$), both noise and signal sources have been connected to the "eigenbased" block inputs (Fig. 10). The primary signal is read from a file containing a segment of DVB-T signal with 8k subcarriers, code rate 5/6, 64-QAM constellation and CP ratio 1/4. The signal is sampled at the nominal rate of 64/7 Msamples/s.

C. Results

The results obtained for the DVB-T signal under linear mixture models provided by flat fading Rayleigh channel are reported in Fig. 3. First, we report the ROC curve then, by setting the false alarm rate to 0.01, we plot the detection probability as a function of the signal-to-noise ratio. By fixing the detection probability, this allows to evaluate the differences in terms of SNR between the algorithms, at the parity of detection and false alarm probability.

Simulations have been performed assuming $K = 10$ antennas and and observation interval corresponding to $N = 50$ samples.

Looking at Fig. 3, we observe that the best algorithm for known noise variance is the RLRT, while GLRT is the best under unknown variance. We note that these results are in agreement with the results provided in the literature for Gaussian signals. As a reference, results for the same algorithms obtained by simulating Gaussian signal samples are reported in Fig. 4 and are essentially identical to the previous ones (as expected, since the Gaussian properties of the DVB-T signal have been verified).

Under a more realistic model, the TU6 channel, the performance of the algorithms are different, as can be observed in Fig. 5. We see how both GLRT and RLRT lose their first place when the received signal model is different from the linear mixture one: simple energy detection becomes highly competitive in this case. The difference between algorithms with known and unknown noise variance is larger, too.

It is important to note that, in this work, we have assumes a perfect knowledge of the noise variance for RLRT, LRT and energy detection. Further analysis will be applied to study their performance under imperfect noise variance knowledge, and address its impact for real DVB-T signals (analysis for Gaussian signals can be found, for example, in [36] for energy detection and [14] for RLRT).

Furthermore, we compare the algorithms for unknown noise variance against the technique exploiting the cyclic prefix autocorrelation of the received signal [5][6] described before. For such method, an interval corresponding to one OFDM symbol has been considered. Moreover, in such case, the signal was sampled at 12.5 Msamples/s. Here, the AWGN channel model is adopted. In this case, we can observe that the performance of this algorithm is similar to that of the GLRT. This single-antenna algorithm does not require the computation of the

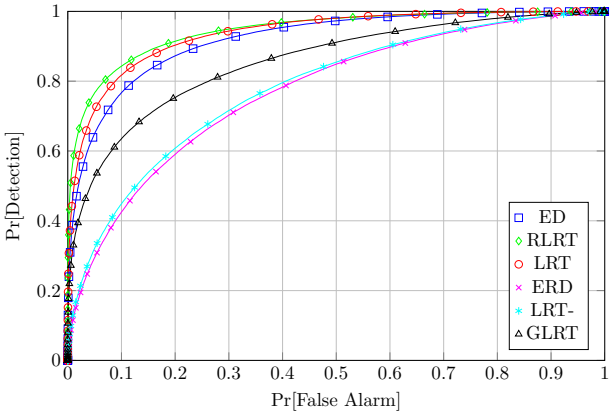

(a) Receiver operating curves (SNR = -10dB).

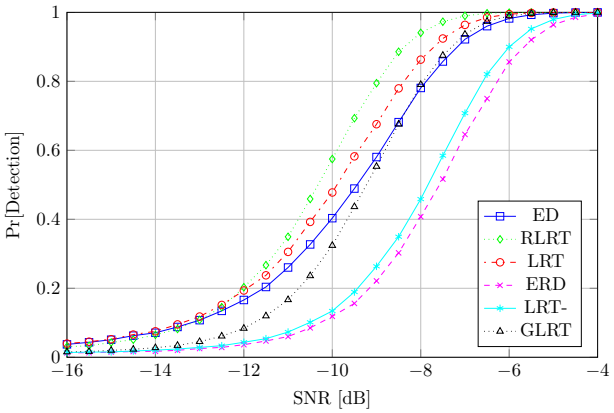

(b) Detection probability.

Fig. 12. DVB-T signal through flat-fading channel with emulated sensors.

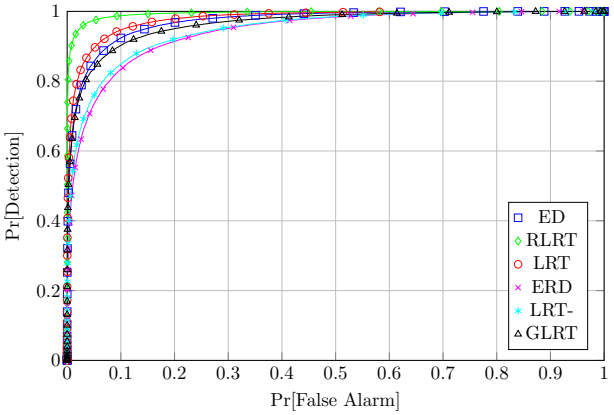

(a) Receiver operating curves (SNR = -10dB).

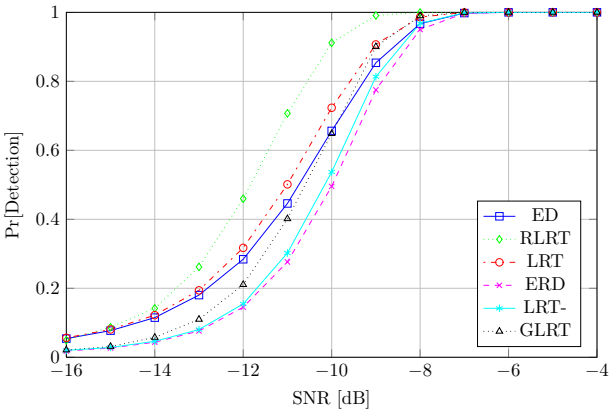

(b) Detection probability.

Fig. 13. DVB-T signal through flat-fading channel, $K = 4$, $N = 200$.

eigenvalues of the sample covariance matrix, but resorts to a precise knowledge of the signal characteristics.

The performance of the proposed feature-based spectrum sensing algorithm has been further evaluated sampling a different number of consecutive OFDM symbols (1, 10, 100 symbols). Considering a constant false alarm probability of 0.1, the curves of Fig. 7 show how the detector sensitivity improves with the number of OFDM symbols. Both in Fig. 6 and Fig. 7 the performance of the CP based method has been estimated using GNU Radio through the procedure described in Sec. VI.

WE also devised a solution for using the eigenbased detectors in a single-antenna scenario. In Fig. 12, corresponding to a flat-fading scenario, $K = 10$ sensors have been emulated through oversampling of a factor K and demultiplexing the received signal stream into K parallel streams. The K demultiplexed and decimated outputs are written in matrix $\boldsymbol{Y}$ so that the generic sample i of the original oversampled signal is stored in row $mod(i, K)$. As it can be noticed, the performance is slightly worse w. r. t. Fig. 3, where the same parameters $N = 50$ and $K = 10$ have been used.

Figs. 13 and 14 show the ROC plot and P_d vs. SNR in a flat fading channel with a different set of paramenters: $K = 4$ and $N = 200$, respectively simulated in a numerical computing environment and in GNU Radio through the flow graphs shown in Figs. 9 and 10. It can be noticed that the results are almost identical, thus validating the correctness of the "eigenbased" block.

Finally, in Fig. 15 we plot the detection probability of GLRT as a function of the observation interval (expressed both in time units and number of received samples per sensor) and the number of sensors for a specific SNR value of -10dB and -15dB, while the false alarm probability remains fixed to 10^{-2}. The channel is Rayleigh flat-fading. As shown, it is possible to obtain the same performance achieved in Fig. 3 using $K = 10$ sensors even with a lower and hence more realistic number of antennas.

VIII. Conclusions

Unused channels in licensed RF bands are one of the most attractive opportunities for secondary cognitive radio systems as long as they enjoy favorable propagation conditions and feature fairly large bandwidths.

In order to avoid interference to PUs while simultaneously performing high-speed communications, TV white-space systems must be equipped with efficient spectrum-sensing procedures.

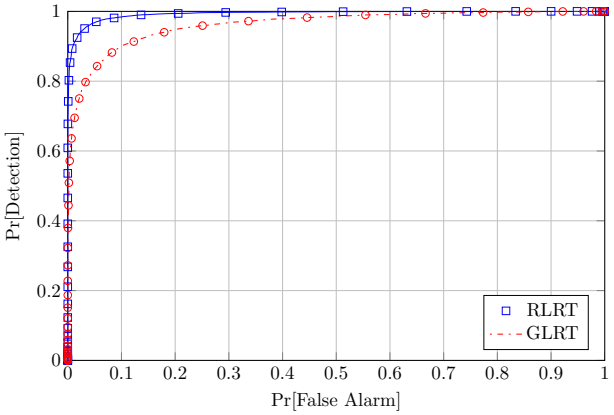

(a) Receiver operating curves (SNR = -10dB).

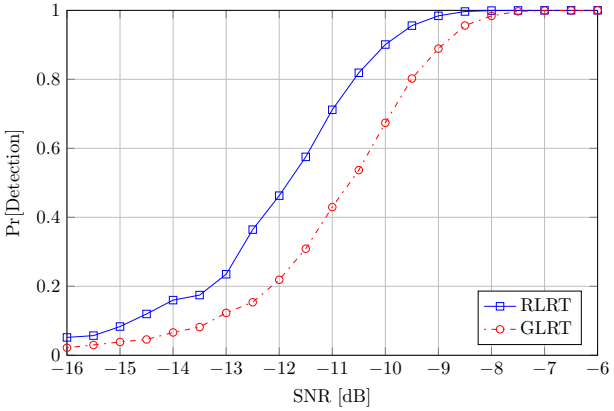

(b) Detection probability.

Fig. 14. DVB-T signal thorugh flat-fading channel, GNU Radio simulation, $K = 4$, $N = 200$.

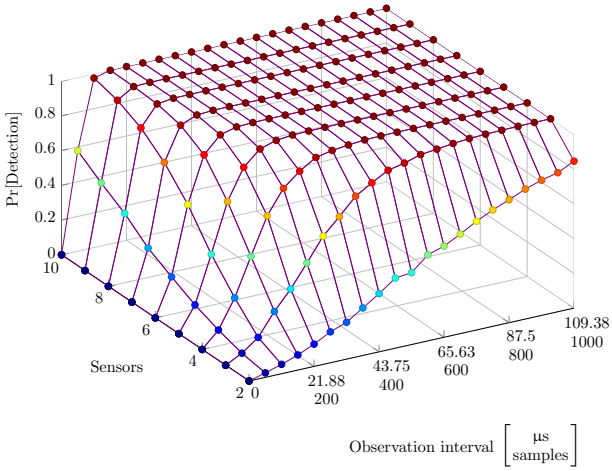

(a) SNR = -10dB, P_{fa} = 0.01.

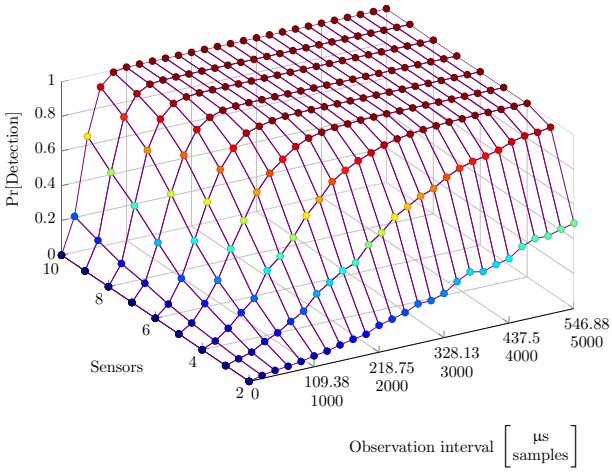

(b) SNR = -15dB, P_{fa} = 0.01.

Fig. 15. GLRT detection probability as a function of time (samples) and sensors through flat-fading channel.

For a large selection of sensing algorithms among the most relevant ones, performance has been assessed applying real DVB-T under different channel profiles: he flat fading channel analysis confirms the results previously obtained by simulation using linear mixture models of Gaussian signals while, under a more realistic multi-path channel model, the performance relationships between the same algorithms is completely different. Simpler algorithms like energy detection becomes highly competitive in this case.

A SDR implementation of an *eigenbased* spectrum sensing detector has been carried out to prove that the complexity of these algorithms is manageable in real-time systems.

Overall, these results show that spectrum sensing algorithms applied to OFDM signals can reach a high accuracy in terms of primary signal detection and false-alarm rate, hence they are well suited for TV white-space secondary networks.

In our research, further effort will be devoted to investigating broader sets of sensing techniques, both with a single antenna and with multiple antennas. Distributed sensing algorithms will be considered as well in order to achieve further improved performance.

REFERENCES

[1] D. Riviello, S. Benco, F. Crespi, A. Perotti, and R. Garello, "Sensing of DVB-T signals for white space cognitive radio systems", *COCORA 2013, The Third International Conference on Advances in Cognitive Radio*, Apr. 2013, pp. 12-17.

[2] J. Mitola, III, "Cognitive radio - an integrated agent architecture for software defined radio," Ph.D. dissertation, Royal Institute of Technology (KTH), May 2000.

[3] S. Haykin, D. J. Thomson, and J. H. Reed, "Spectrum sensing for cognitive radio," *Proceedings of the IEEE*, , May 2009, Vol. 97, No. 5, pp. 849-877.

[4] Y. Zeng, Y.-C. Liang, A. T. Hoang, and R. Zhang, "A review on spectrum sensing for cognitive radio: challenges and solutions," *EURASIP Journal on Advances in Signal Processing*, Jan. 2010, pp. 1-15.

[5] S. Benco, F. Crespi, A. Ghittino, and A. Perotti, "Software-defined white-space cognitive systems: implementation of the spectrum sensing unit", in *The 2nd Workshop of COST Action IC0902*, Oct. 2011, pp. 1-3.

[6] D. Danev, E. Axell, and E. G. Larsson, "Spectrum sensing methods for detection of DVB-T signals in AWGN and fading channels," in *Proc. IEEE 21st International Symposium on Personal Indoor and Mobile Radio Communications (PIMRC)*, Sep. 2010, pp. 2721-2726.

[7] K. Manolakis, D. M. Gutiérrez Estévez, V. Jungnickel, W. Xu, and C. Drewes, "A closed concept for synchronization and cell search in 3GPP LTE systems," *IEEE Wireless Communications and Networking Conference (WCNC 2009)*, Apr. 2009, pp. 1-6.

[8] F. Crespi, M. Maglioli, A. Perotti, and S. Benco, "A real-time video broadcasting system based on the GNU Radio-USRP2 platform", *Proc. Karlsruhe Workshop on Software Radios (WSR)*, Mar. 2012.

[9] European Telecommunications Standards Institute, "ETSI EN 300 744, digital video broadcasting (DVB); framing structure, channel coding and modulation for digital terrestrial television," Jan. 2009.

[10] COST207, "Digital land mobile radio communications (final report)," Commission of the European Communities, Directorate General Telecommunications, Information Industries and Innovation, Tech. Rep., 1989.

[11] J. Neyman and E. Pearson, "On the problem of the most efficient tests of statistical hypotheses", *Philosophical Transactions of the Royal Society of London*, 1933, Series A, vol. 231, pp. 289-337.

[12] P. Bianchi, M. Debbah, M. Maida, and J. Najim, "Performance of statistical tests for single-source detection using random matrix theory", *IEEE Transactions on Information Theory*, 2011, pp. 2400-2419.

[13] Q. Zhang, "Advanced detection techniques for cognitive radio", in *Proc. of International Conference on Communications (ICC 2009)*, Jun. 2009, pp. 1-5.

[14] B. Nadler, F. Penna, and R. Garello, "Performance of eigenvalue-based signal detectors with known and unknown noise level", in *Proc. of International Conference on Communications (ICC 2011)*, Jun. 2011, pp. 1-5.

[15] S. N. Roy, "On a heuristic method of test construction and its use in multivariate analysis", *Annals of Mathematical Statistics*, Jun. 1953, vol. 24, no. 2, pp. 220-238.

[16] L. Wei and O. Tirkkonen, "Cooperative spectrum sensing of OFDM signals using largest eigenvalue distributions", in *IEEE International Symposium on Personal, Indoor and Mobile Radio Communications (PIMRC 2009)*, Sep. 2009, pp. 2295-2299.

[17] S. Kritchman and B. Nadler, "Non-parametric detections of the number of signals: hypothesis testing and random matrix theory," *IEEE Transactions on Signal Processing*, Oct. 2009, Vol. 57, No. 10, pp. 3930 -3941.

[18] J. Baik and J. W. Silverstein, "Eigenvalues of large sample covariance matrices of spiked population models",*J. Mult. Anal.*, 2006, vol. 97, no. 6, pp. 1382-1408.

[19] F. Penna, R. Garello, and M. A. Spirito, "Probability of missed detection in eigenvalue ratio spectrum sensing", in *5th IEEE International Conference on Wireless and Mobile Computing, Networking and Communications (WiMob)*, Oct. 2009, pp. 117-122.

[20] H. Urkowitz, "Energy detection of unknown deterministic signals", *Proceedings of the IEEE*, Apr. 1967, vol. 55, no. 4, pp. 523-531.

[21] P. Bianchi, J. Najim, G. Alfano, and M. Debbah, "Asymptotics of eigenbased collaborative sensing", in *Proc. IEEE Information Theory Workshop (ITW 2009)*, Oct. 2009, pp. 515-519.

[22] G. V. Moustakides, "Finite sample size optimality of GLR tests", *IEEE Transactions on Information Theory*, Nov. 2009, pp. 1-20.

[23] Y. H. Zeng and Y.-C. Liang, "Eigenvalue based spectrum sensing algorithms for cognitive radio", *IEEE Transactions on Communications*, Jun. 2009, Vol. 57, No. 6, pp. 1784-1793.

[24] W. J. Krzanowski, *Principles of multivariate analysis: a user's perspective*. Oxford University Press, 2000.

[25] J. W. Mauchley, "Significance test for sphericity of a normal n-variate distribution", *Annals of Mathematical Statistics*, Jun. 1940, vol. 11, no. 2, pp. 204-209.

[26] J. Mitola, III, "Software radios-survey, critical evaluation and future directions",*IEEE Aerospace and Electronic Systems Magazine*, 1993,vol. 8, no. 4, pp. 25-36.

[27] GNU Radio. [Online]. Available:http://gnuradio.org 06.12.2013

[28] W. E. Arnoldi, "The principle of minimized iterations in the solution of the matrix eigenvalue problem", *Quarterly of Applied Mathematics*, 1951, vol. 9, pp. 1729.

[29] M. T. Jones and M. L. Patrick, *The use of Lanczos's method to solve the large generalized symmetric definite eigenvalue problem*, Defense Technical Information Center, 1989.

[30] J. K. Cullum and R. A. Willoughby, *Lanczos algorithms for large symmetric eigenvalue computations: Vol. I: Theory*, SIAM, 2002.

[31] C. Guo and S. Qiao, "A stable Lanczos tridiagonalization of complex symmetric matrices", *Advanced Signal Processing Algorithms, Architectures, and Implementations XV, Proc. of SPIE*, 2005, pp. 1-12.

[32] J. Kuczynski and H. Wozniakowski, "Estimating the largest eigenvalue by the power and Lanczos algorithms with a random start", *SIAM Journal on Matrix Analysis and Applications*, Oct. 1992, vol. 13, no. 4, pp. 1094-1122.

[33] W. Barth, R. S. Martin, and J. H. Wilkinson, "Calculation of the eigenvalues of a symmetric tridiagonal matrix by the method of bisection", *Numerische Mathematik*, 1967, Vol. 9, pp. 386-393.

[34] D. J. Evans, J. Shanehchi, and C. C. Rick, "A modified bisection algorithm for the determination of the eigenvalues of a symmetric tridiagonal matrix", *Numerische Mathematik*, 1982, Vol. 38, pp. 417-419.

[35] G. Verma and P. Yu, "Developing signal processing blocks for software-defined radios", *Adelphi, MD : Army Research Laboratory*, Jan. 2012.

[36] R. Tandra and A. Sahai, "SNR walls for signal detection", *IEEE Journal of Selected Topics in Signal Processing*, Feb. 2008, vol. 2, no. 1, pp. 4-17.